Increase ACE2 Concentrations Embedded in the Memristive Electrochemical Sensor Membranes Promote Direct Reagent-free Sensing of S1 Antigen of SARS-Cov2 Virus

E. T. Chen[*], J. T. Thornton[**], S-H. Duh[***]

[*]Advanced Biomimetic Sensors, Inc., 6710A Rockledge Drive,
Bethesda, MD 20817, USA, ellen@abs-isensors.com
[**] Bruker Nano, 19 Fortune Dr., Billerica, MA 01821, USA
[***]University of Maryland Medical System, 22 South Greene St, Baltimore, MD 21201, USA

ABSTRACT

We developed three S1 Cov19 antigen sensors with embedded ACE2 concentrations from 4.5, 57.5 to 230 nM cross-linked with multiple copolymers formed self-assembled membranes under antibody-free conditions for sensors 1, 2, and 3, respectively for fast testing and monitoring of a single S1 particle SARS-CoV-2 virus in 120s, which is suitable for testing asymptomatic patients with higher than 92±9% to 96±4% accuracy using spiked 40 aM fasting human saliva specimens against the results from the calibration curves by the DSCPO and OPO method, respectively. Low ACE2 concentration embedded in sensor 1 has the results of reversed potential membrane (RPM) indicator of the ratio of Ap/Rp located in the unsafe zone, while sensor 2 and 3 kept in the normal zone. Accuracy results are 99 ± 2% using spiked S1 60 nM in NIST SRM965 human serum compared with that of the data from calibration. The imprecision results are 1.96% over the linear range from 0.1 nM to 100 nM (n=12, $p<0.0001$); the imprecision result of the single virus particle has an RSD 0.1% related to the mean over the concentration range from 5 aM to 100 pM (n=18, $p<0.0001$) using the OPO method.

***Keywords*:** S1 Antigen Memristive Sensor; Reversible Membrane Potential; Ratio of Action Potential/Resting Potential, Antibody-free sensing.

1. INTRODUCTION

Serological and immunological assay methods are widely used for the analysis of the presence of immunoglobulin (IgM) or IgG antibodies in blood serum or testing in posterior oropharyngeal saliva for public screening testing during the Covid 19 pandemic [1-3]. Spike (S) protein has been a well-known target antigen of the SARS-CoV-2 virus, that first attacks human angiotensin-converting enzyme 2 (ACE2) receptor-binding domain (RBD), then mediating entry into human cells [4-7]. Fast and precise detection of the presence of SARS-CoV-2 virus using the gold standard of reverse transcription-polymerase chain reaction (RT-PCR) is very challenging in order to meet the urgent needs, due to the performance limitations of the instrumentation, expensive reagents, long time waiting for results, and protein interference [1-4]. The *American Society for Microbiology COVID-19 International Summit* had suggested further improving the testing of SARS-CoV-2 viral antigens considered to deserve further research for Point-of-Care (POC) facilities to test asymptomatic patients [8]. Another call from the article revealed the fact that there is a worldwide shortage of reagents to perform the detection of SARS-CoV-2. Many clinical diagnostic laboratories rely on commercial platforms that provide integrated end-to-end solutions. While this provides established robust pipelines, there is a clear bottleneck in the supply of reagents given the current situation of extraordinarily high demand [9]. In an attempt to respond to urgent calls and to fulfill the unmet needs, our goal of this research is to develop a hand-hold electrochemical S1 antigen sensor for fast, accurate sensing and monitoring of single-particle SARS-CoV-2 virus in human biological specimens under reagent-free, label-free and antibody-free conditions.

Our approaches to reach our goals are:1) immobilizing ACE2 cross-linked with organic conductive co-polymers to form a self-assembled membrane on bare gold chips; 2) changing ACE2 concentration to three levels in 4.5, 57.5 to 230 nM for sensors 1, 2, and 3, respectively to study the immobilized ACE2 concentration impacting on the S1 antigen communication with the sensor; 3) using an open circuit potential method and a double step chronopotential (DSCPO) method to study S1 antigen concentration change impact the OPO energy level and the cell reversible membrane potential (RMP) change in a short monitoring time in the presence ACE2 under reagent-free and antibody-free, tracer-free conditions compared with controls.

2. RESULTS AND DISCUSSIONS

2.1 The ACE2 Concentration Impacts the Structure of the SAMs

Fig. 1A, 1B and 1C depict the thickness of the SAM in the AFM images having a positive correlation with the concentrations of the immobilized ACE2 in the order of

Sensor 3's membrane thickness > sensor 2> sensor 1 in the presence of ACE2 from 230 nM > 57.5 nM >4.5 nM.

The ACE2 is a multiple function enzyme comprising of a C-terminal region (carboxy domain), N-terminal peptide region and an HEXXH zinc finger metalloprotease motif (catalytic domain) [10-15]. Paul Towler's group's x-ray structure revealed the native ACE2 formed a zinc finger comprising of His^{374}, His^{378} Glu^{402}, one water molecule, and coordinated with Zn^{+2}at the active site [13-15]. Sensor 3 shown high surface roughness with more nanostructure bumps, and small balls in the membrane in Fig. 1C than sensor 2 of Fig 1B and sensor 1 of Fig 1A. Our work used ACE2 cross-linked with triacetyl-ß-cyclodextrin (TCD), polyethylene glycol diglycidyl ether (PEG) and poly(4-vinylpyridine) (PVP) has enriched the zinc-finger from ACE2 and associated with the catalytic subdomain α-helix from the PEG and the PVP, and the COO^- of the TCD further enriches Glu^{402}'s function evidenced by the increased ACE2 in the SAMs showed a transformed surface with densely packed large nano-bumps and small nano-balls.

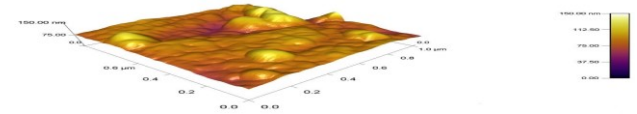

Fig. 1A

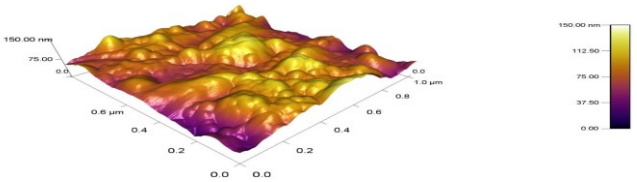

Fig. 1B

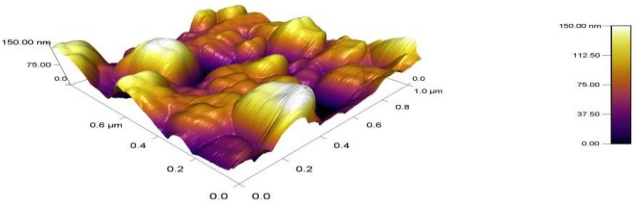

Fig. 1C

2.2 S1 Antigen Impacts on the Three Sensors in the Open Circuit Potential

Sensor 1 has the lowest embedded ACE2 exhibiting with the lowest slope of the sensitivity in the plot of the potential vs. time curve compared with Sensor 2 and Sensor 3 shown in Fig. 2A. Fig. 2B shows in the 40 aM S1 antigen, the trend of the open circuit potential decrease rate to the negative value is in the order sensor 1>sensor 2>sensor 3, that indicates elderly who has lower ACE2 in the tissue having lower energy compared with the youth who has higher energy before S1 attacks, and when S1 attacks, sensor 1 has the lowest negative energy.

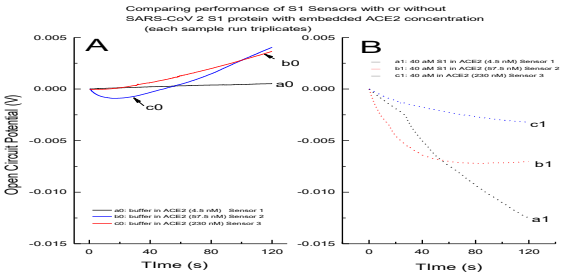

Fig. 2 depicts the open circuit potential curves vs. 120s in the buffer compared with three sensors. Fig. 2B shows the open circuit potential curves in the 40 aM S1 antigen.

2.3 Quantitation of S1 SARS-CoV-2 Virus

2.3.1 S1 Antigen at Low and High Concentration Levels Impact on Sensor 1 Energy

Sensor 1 has the lowest imbedded ACE2 of 4.5 nM among other sensors, therefore we chose sensor 1 to study the S1 antigen concentrations impact on the cell energy in a low and high end. Fig. 4 depicts the results of S1 of 40 aM reduced the cell equilibrium energy from the buffer controls of 0.514 ± 0.003 mV, down to -12.43 ± 0.04 mV (22-fold decreased); and the 240 nM S1 antigen reduced the energy from positive 0.514 mV to -25.4 ± 0.07 mV (37-fold decrease) as shown in Fig. 3 using the OPO method of monitoring the energy change in 120s compared with the controls.

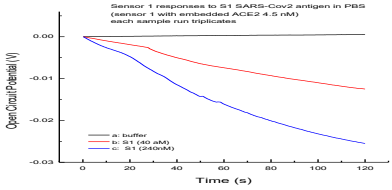

Fig. 3 depicts the S1 antigen impact cell energy on Sensor 1 compared with the PBS controls (all samples run triplicates).

2.3.2 The Calibrations

Sensor 3 has the highest embedded ACE2 and was chosen for the S1 impacting cell equilibrium energy study. Fig. 4 (L) shows Sensor 3 has the highest initial cell energy of 31.3 ± 0.16 mV in the buffer, and the energy was inversely decreased as the S1 concentration increased from 5 aM to 100 pM of 6 levels compared with controls, and the negative energy started appear at 100 fM. Fig. 4 (R) depicts S1 concentrations inversely impact sensor 3's energy at the higher end over 0.1 nM to 120 nM of 4 levels. Fig. 5 (L) depicts the calibration curve at the low end of S1 concentration vs. OPO potential compared with the controls. It produced a log regression equation Y (mV) = -0.877-0.51 Log X, r= -0.986 (n=18), P<0.0001, Sy/x=0.22

over S1 concentration 5.0 aM to 100 pM having an imprecision of the single virus particle of 0.1%. The Detection of Limits (DOL) is 0.19 aM. Fig. 5 (R) depicts the calibration curve at the high end. It produced a linear regression equation Y (mV) = -1.15 + 0.1 X, r= -0.992 (n=12), P<0.0001, Sy/x= 0.71 over S1 concentration 0.1 nM to 120 nM with a DOL 0.5 nM having an imprecision of 1.96%.

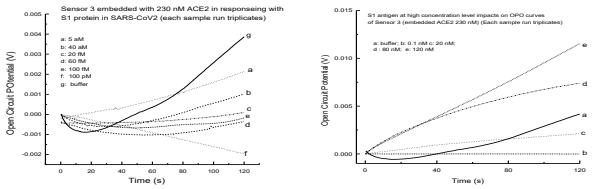

Fig. 4 (L) depicts Sensor 3's OPO potential vs. time curves over S1 5 aM to 100 pM. Fig. 4 (R) depicts the plots at the high concentrations from 0.1 to 120 nM.

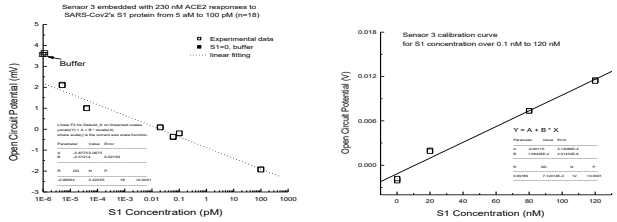

Fig. 5 (L) and 5 (R) depict the calibration curves over the low and high S1 concentrations.

2.4 The Imprecision and Accuracy Using Biological Specimens by the OPO Method

Multiple groups suggested to use salivary samples for testing SARS-CoV-2 [3, 11], because of the easiness for self-collected sample with almost no discomfort. Our human fasting saliva samples with or without spiked 40 aM S1 antigen were used for the recovery study and results showed the recovery rate (accuracy) is 96 ± 4%. The recovery results showed 99 ± 2% using the NIST SRM965 human serum with a certified glucose 300 mg/dL as the control, compared with spiked S1 antigen 60 nM in the serum by the OPO method.

2.5 Quantitation of S1 Antigen of SARS-CoV-2 by a Double-step Chronopotentiometry (DSCPO) Method

2.5.1 The Calibration Curve

Fig. 6 depicts the curves of voltage vs. time at ±10 nA over 40 pM to 120 nM S1 antigen concentrations against the control samples with each sample run triplicates using Sensor 3. Fig. 7 depicts the calibration curve of the cell voltage vs. S1 antigen concentrations, and it produced a first-order exponential decay equation by an Exponential Decay regression of y = A1*exp(-x/t1) + y0 with y= 0.017*exp(-x/36) +0.016, and the Chi^2/DoF= 5.9407E^{-6} (n=15).

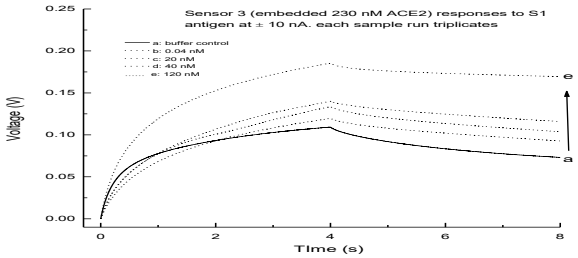

Fig. 6 depicts the voltage vs. time curves at ± 10 nA over S1 antigen concentrations 0.04 nM-120 nM with each sample run triplicates by the DSCPO method.

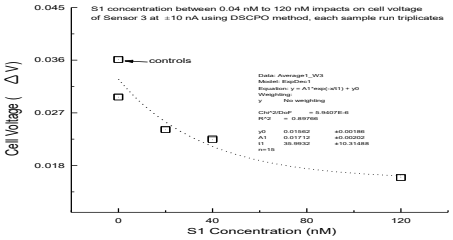

Fig. 7 depicts the plot of cell voltage vs. S1 concentration using the DSCPO method.

2.5.2 The Imprecision and Accuracy Using Biological Specimens by the DSCPO Method

The fasting salivary samples were collected from a healthy subject. The point imprecision and accuracy were assessed by the recovery study. The results showed the recovery rate is 92.3 ± 9% by spiked S1 antigen 40 aM samples against the saliva controls after corrected the factor between the saliva controls and the buffer controls. The recovery results showed 118 ± 0.2% using the NIST SRM965 human serum with a certified glucose 300 mg/dL as the control, compared with spiked S1 antigen 60 nM in the serum by the DSCPO method.

2.5.3 Assessing S1 Concentration Ranges Effecting on Cell Reversible Membrane Potential (RMP)

Researchers reported many diseases unable to maintain mitochondrial cell's RMP, and a biomarker of the potential ratio of Action potential (Ap) vs. resting potential (Rp) found is an indicator that direct correlating with the RPM [21-26]. Fig. 8 depicts sensor 1 has results located in the unsafe zone compared with other sensors by using the DSCPO method.

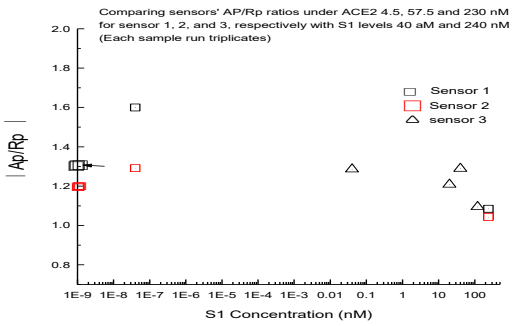

Fig. 8 depicts the Ap/Rp ratio results vs. S1 concentrations.

2.6 Comparing the Spiked S1 Antigen Impacting on the i-V Curves Using the Fasting Saliva

Memristors and Memcapacitors are devices made of nanolayers that remember the past event, and mimic neuronal synapse with a hysteresis loop in the i-V curve [16-20]. Comparison of the impacts of the single particle S1 of Covid-19 antigen on the i-V curves at scan rate 1 Hz (Slow-Wave Sleep (SWS)) vs. controls from the three sensors as shown in Fig 9 (L) and Fig. 9 (R), indicates sensor 1 is most vulnerable to S1 attack at SWS shown the signature peak at -0.4V (w/o S1) was moved to -0.6V increased 6-fold the peak intensity in the presence 40 aM S1. Sensor 2 and Sensor 3 behave better when facing the S1 antigen attack, because of no signature peak occurred. In Fig. 9 (L) sensor 3 shows the perfect memristive loop with cross point at zero-bias, and has almost 10-times peak intensity due to the high embedded ACE2 230 nM, compared with sensor 1 and 2.

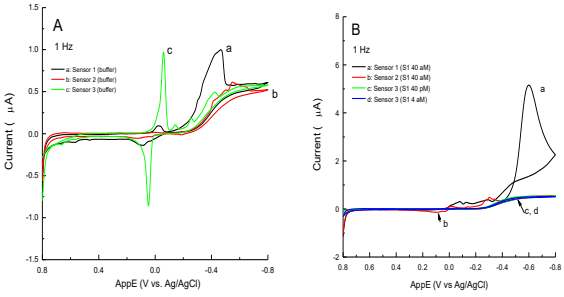

Fig. 9 (L) depicts the control i-V curves in PBS solution at 1 Hz for three sensors. Fig. 9 (R) depicts the S1 impacts on the sensors' i-V curves.

3. EXPERIMENTAL

The Self-Assembled Membrane (SAM) was fabricated by a mixture solution of copolymers cross-linked with triacetyl-ß-cyclodextrin (TCD), polyethylene glycol diglycidyl ether (PEG) and poly(4-vinylpyridine) (PVP) and ACE2 with an appropriate composition deposited on a gold chip with Ag/AgCl as the reference electrode, and incubated for 72 hours at 37°C. The ACE2 concentration embedded was 4.5, 57.5 and 230 nM for sensor 1, 2 and 3, respectively. The morphology of the AU/SAM was characterized using an Atomic Force Microscope (AFM) (Asylum).

The S1 (1-681, MW76 kDa, recombined) antigen of SARS-CoV-2 was heat inactive and was purchased from Axxora, NY11735. The fasting human saliva specimens were collected from healthy subjects under Board approval. The NIST SRM 965 human serum were purchased from NIST, Gaithersburg.

4. CONCLUSION AND DISCUSSIONS

We demonstrate a handhold prototype device with an ACE2 embedded SAM promoted direct reagent-free and antibody-free fast testing and monitoring of a single S1 particle SARS-CoV-2 virus in 120 s, which is suitable for testing asymptomatic patients with higher than 92±9% to 96±4% accuracy using spiked 40 aM fasting human saliva specimens against the results from the calibration curves by the DSCPO and the OPO method, respectively. Low ACE2 concentration embedded in sensor 1 has the results of RPM indicator of the ratio of Ap/Rp located in the unsafe zone, while sensor 2 and 3 kept in the normal zone. An increase ACE2 concentration in the SAM preventing S1 virus drainage of the cell energy is demonstrated. Further selectivity study among different SARS-CoV-1 and CoV- 2 is needed. Comparing with the enzyme-linked immunosorbent assay (ELISA) method is needed for verifications.

ACKNOWLEDGEMENT

We thank the University of Maryland Nano Analysis center for the AFM images. E. Chen thanks Dr. Karen Geskell for her help and valuable discussions.

REFERENCES

Please see www.ABS-isensors.com